Solutions to the Droplet Collection Equation for Polynomial Kernels

ALEXIS B. LONG[1]

Division of Cloud Physics, CSIRO, Sydney, Australia

(Manuscript received 5 November 1973)

ABSTRACT

Numerical solutions to the droplet collection equation, using certain polynomial approximations to the gravitational collection kernel, are examined to learn whether they usefully describe the evolution of a cloud droplet size distribution. The results for typical continental and maritime clouds show that the distribution is closely described if the kernel is replaced by

$$9.44\times10^{9}(x^2+y^2),\ R\leqslant 50\ \mu\text{m};\qquad 5.78\times10^{3}(x+y),\ R>50\ \mu\text{m},$$

or by

$$1.10\times10^{10}x^2,\ R\leqslant 50\ \mu\text{m};\qquad 6.33\times10^{3}x,\ R>50\ \mu\text{m},$$

where R is the radius of the larger droplet, x its volume in cubic centimeters, and y the volume of the smaller droplet.

From the standpoint of including collision and coalescence of droplets in multi-dimensional cloud models an *analytic* solution to the collection equation is desirable. An attempt should be made to find such solutions based upon either of the above approximations. If these cannot be found because of the piecewise nature of the approximations, then solutions based on the portions for $R\leqslant 50\ \mu$m would still describe the first few hundred seconds of droplet growth. A comparatively poor description of the droplet distribution comes from the most physically realistic analytic solution presently existing, based on the kernel approximation $B(x+y)+Cxy$.

1. Introduction

Satisfactory inclusion of droplet collision and coalescence in a theoretical cloud model requires knowing their effect on the spectral distribution function $n(x,t)dx$. This gives at time t the mean number density of droplets with individual volumes x to $x+dx$. The function $n(x,t)$ is obtained by solving a scalar transport "collection" equation of the form

$$\frac{\partial n(x,t)}{\partial t}=\int_0^{x/2} n(x-y,t)K(x-y,y)n(y,t)dy - n(x,t)\int_0^{\infty} K(x,y)n(y,t)dy. \quad (1)$$

The first integral represents the increase in $n(x,t)$ expected because of the binary collision and coalescence (collection) of droplets whose volumes $x-y$ and y sum to the volume x. The second integral represents the decrease in $n(x,t)$ expected because of binary collision and coalescence of x-droplets with larger and smaller ones. The stochastic nature of the droplet collection process enters (1) through the collection kernel $K(x,y)$. This quantity is related to the probability that in a given interval of time there will be in a cloud a collection event involving two particular droplets of volumes x and y. Derivations and discussions of (1) can be found in Twomey (1964, 1966), Berry (1965, 1967, 1968), Scott (1967, 1968b, 1972), Warshaw (1967, 1968a), Long (1971, 1972a, b) and Gillespie (1972).

Solutions to (1) have been either numerical or analytic depending upon the form of $K(x,y)$. Numerical solutions (Twomey, 1964, 1966; Berry, 1965, 1967; Warshaw, 1967, 1968b) have been based upon a gravitational collection mechanism, for which the kernel is

$$K(x,y)=\pi[R(x)+r(y)]^2E(x,y)[V(x)-V(y)],\qquad x\geqslant y, \quad (2)$$

where $R(x)$ is the radius of the larger collector droplet, and $r(y)$ is the radius of the smaller collected droplet (both droplets are assumed to be spherical); $E(x,y)$ is the collection efficiency of the two droplets and is given by the product of their collision efficiency $E_c(x,y)$ and coalescence efficiency $E_s(x,y)$; and V is the droplet terminal fall velocity. Analytic solutions to (1) have been obtained, principally by Melzak (1953), Golovin (1963a), Scott (1968a), and Drake and Wright (1972), for approximations to K given by the polynomials:

$$P(x,y)=A \quad (3a)$$

$$P(x,y)=B(x+y) \quad (3b)$$

$$P(x,y)=Cxy \quad (3c)$$

[1] Present affiliation: Cooperative Institute for Research in Environmental Sciences, University of Colorado, Boulder.

$$P(x,y)=A+B(x+y) \tag{3d}$$

$$P(x,y)=B(x+y)+Cxy \tag{3e}$$

$$P(x,y)=A+B(x+y)+Cxy, \quad A=B^2/C. \tag{3f}$$

This paper examines how well these and certain other polynomials approximate $K(x,y)$ and how well solutions to (1) based on them correspond to numerical solutions based on K. A close correspondence would justify replacing the numerical solutions by analytic solutions based on the polynomials.

This investigation is important because numerical solutions to (1) have a limited utility, especially if they are to be incorporated, along with the predictions of other cloud physical equations, into an overall description or model of a cloud. For instance, a numerical solution appears in tabular form. Its use in other cloud physical equations is thus complicated. The numerical computation time required to obtain $n(x,t)$ throughout a cloud model is given as the time required at any point in the model ($\sim$0.1–10% real time) multiplied by the number of its grid points ($\sim 10^3$–10^6). The computation time is then prohibitive.

With these drawbacks to numerical solutions in mind two alternative methods for solving (1) have been proposed. Bleck (1970) has developed an approximate numerical method for solving (1) based on using in place of $n(x,t)$ its x-weighted mean value over a small interval about x. This is supposed to require less computer time than a direct numerical solution. The time on a CDC 6600 computer actually involved for Bleck's calculation is 11 msec per iteration, which is not appreciably smaller than the 13 msec per iteration required by Berry (1967) in his early numerical solutions to (1). Later numerical solutions have required more time as the techniques for approximating the integrands in (1) have become more sophisticated (Reinhardt, 1972), but these later solutions are also considerably more accurate. It is doubtful whether the approximate solutions of Bleck are accurate descriptions of droplet growth, especially in the "tail" of the distribution, where we find those large drops which are all-important in the development of precipitation. We also note that Bleck's method yields only a tabular version of the size distribution.

Drake (1972) has discussed a method for solving (1) by expressing $n(x,t)$ in terms of its statistical moments $M_i(t)$, $i=0, 1, 2, \ldots$. This was proposed earlier by Golovin (1963b, c, 1965) and Enukashvili (1964a, b), and has been discussed by Long (1972b, p. 48); in principle, it yields a closed expression for $n(x,t)$ even for a kernel as complicated as that in (2), once the time-dependence of a number of the moments is obtained. The number of moments required to reproduce the distribution is not known, but for an accurate description of the tail region it may be so high as to require the moments to be obtained numerically. This takes us back to the tabular problem associated with numerical solutions to (1).

Up to now analytic solutions to (1) have not been proposed as possible replacements to numerical solutions because the "polynomial" kernels in (3) for which they are valid do not seem to be close approximations to the actual kernel. Nevertheless, the analytic solutions are all algebraic functions of x and t, albeit complicated ones, and are simply evaluated by performing certain straightforward sums. This suggests they might be usefully incorporated into cloud models, provided they correspond closely with numerical solutions.

This paper examines whether there is a close correspondence between the solutions. First, we determine how well each polynomial $P(x,y)$ in (3) matches $K(x,y)$ in (2). We obtain those values of the coefficients A, B and C which minimize the deviation (defined in a certain sense) between K and the respective polynomial P. Comparing this minimum deviation for the various polynomials will tell us which are closest to the actual kernel and most likely to lead to realistic analytic solutions to (1) as compared to actual, numerical solutions. A numerical integration of (1), using in place of K the best polynomials in (3), will show how realistic these solutions are.

Certain polynomials other than those in (3) also are considered and their coefficients evaluated. These polynomials turn out to be closer to K, and it will be suggested that analytic solutions to (1) be sought for them. This will be supported by a numerical integration of (1), using them in place of K, which will show a behavior for $n(x,t)$ remarkably close to that given by numerical solutions based on K itself.

2. Evaluation of $K(x,y)$

The first step in obtaining the coefficients A, B and C in the polynomials $P(x,y)$ is to evaluate the actual kernel $K(x,y)$ in (2).

The collision efficiency for any droplet pair is computed from the efficiencies for particular droplet pairs calculated by Shafrir and Gal-Chen (1971) and by Klett and Davis (1973). These workers give $E_c(R,r)$ for various R between 10 and 300 μm and for most values of $0 \leqslant r \leqslant R$. For droplet pairs within the range of their calculations E_c is here obtained by interpolating on their results. Otherwise, E_c is obtained with extrapolation techniques, except for $R>400$ μm, where it is set equal to unity.

The coalescence efficiency is taken as unity because that knowledge of it which presently exists (Woods and Mason, 1964; Whelpdale and List, 1971; Brazier-Smith *et al.*, 1972) covers only a limited range of droplet pairs.

The terminal velocity is evaluated using the approximate formula developed by Long and Manton (1974). This formula is based on the data of Gunn and Kinzer (1949) and Beard and Pruppacher (1969) obtained at 1013 mb and 20C. An altitude correction to

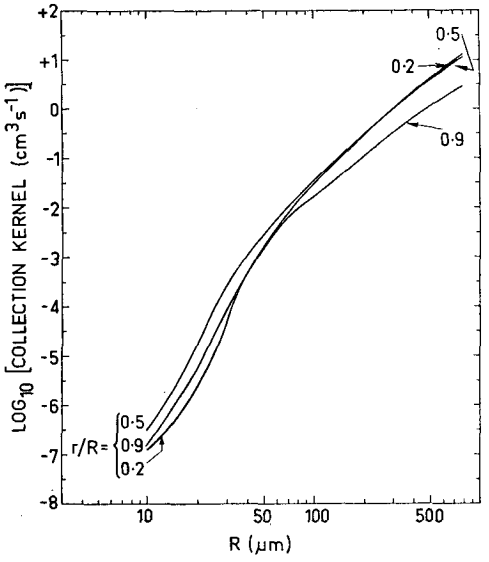

FIG. 1. Actual droplet-collection kernel $K(x,y)$.

the formula is made because the collision efficiencies of Klett and Davis (1973) and Shafrir and Gal-Chen (1971) are for 900 mb and 0C. For droplets <15 μm this correction is derivable from the Stokes terminal velocity formula and is due to the change in the dynamic viscosity of air with temperature. For droplets >1690 μm the correction of Foote and du Toit (1969) is applied. For intermediate droplets a linear interpolation with respect to the logarithm of the droplet radius is used.

Fig. 1 displays representative values of the collection kernel evaluated in the above manner.

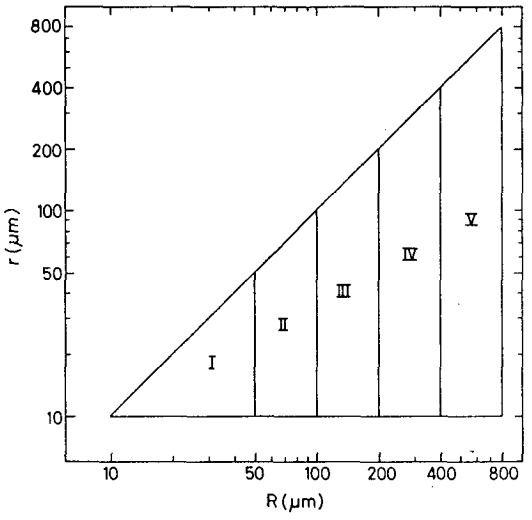

FIG. 2. The five droplet-pair domains over which the polynomials $P(x,y)$ approximate the collection kernel $K(x,y)$. Domain I is as outlined, domain II includes domain I *plus* the additional area denoted by the roman numeral II, domain III includes domain II *plus* the additional area denoted by the roman numerial III, etc.

3. Obtaining the approximating polynomials

There have been two previous determinations of the coefficients A, B and C in (3). Golovin (1963a) evaluated the quotient $K(x,y)/(x+y)$, found it held fairly constant at a value $B\approx 6000$ sec^{-1} for a wide range of $R\gtrsim 50$ μm, and concluded that for these droplets $B(x+y)$ is a reasonable approximation to $K(x,y)$. For smaller R, this approximation is too large by up to an order of magnitude, and here the technique (Scott, 1968a) has been to require the coefficients in any approximating polynomial to be such that it coincides with K for $R=30$ μm and $r=10$ μm.

The coefficients in each approximating polynomial are here obtained by requiring that the rms deviation $D(P;K)$ between the logarithm of $P(x,y)$ and the logarithm of $K(x,y)$ be a minimum. In particular, it is required that

$$D(P;K) \equiv \left[\frac{\int_S\int[\ln P(x,y)-\ln K(x,y)]^2 d(\ln y)d(\ln x)}{\int_S\int d(\ln y)d(\ln x)}\right]^{\frac{1}{2}} \quad (4)$$

be a minimum.

For reasons of accuracy the deviation between the logarithm of $P(x,y)$ and the logarithm of $K(x,y)$ is minimized rather than the deviation between the functions themselves. If this were to be minimized, the increase in $K(x,y)$ of several orders of magnitude that is observed from small to large R (see Fig. 1) would lead to a polynomial depending almost exclusively on K at large R and very little on K at small and medium R. For similar reasons the integration in (4) is carried out with respect to the logarithm of x and y rather than with respect to x and y themselves.

The integration domain S will depend on when in the history of a droplet population the polynomial $P(x,y)$ is approximating $K(x,y)$. Inasmuch as $P(x,y)$ is limited in how well it approximates $K(x,y)$, it seems advisable when obtaining a solution to (1) based on $P(x,y)$ to use for small t (when all droplets are small) a version of the polynomial fitted to values of the kernel for these droplets alone, and to use for longer t (when there are more large droplets) a version of the polynomial taking more into account their kernel. Fig. 2 displays the five domains S used here over which distinct versions of each polynomial $P(x,y)$ are fitted to $K(x,y)$. For small t the solutions to (1) obtained here are based on the domain I version of $P(x,y)$, but as time passes and large droplets are created the solutions are based on versions for domains II, III, etc.

The criterion for changing from one version of P to the next derives from the requirement that the solution to (1) give a good description of the size of the 100th-largest drop per cubic meter of cloud. Since there

are around 100 drops per cubic meter in moderate rain, the size of the smallest of these, $x_{100}(t)$, will tell us how fast precipitation is being produced by collision and coalescence. Furthermore, because the larger drops through their larger kernels have the greatest effect on the entire distribution, accurate knowledge of their sizes will in turn improve the overall solution to (1). The 100th-largest drop grows approximately continuously, at the rate

$$\frac{dx_{100}(t)}{dt}=\int_0^{x_{100}(t)} P[x_{100}(t),y]n(y,t)dy. \tag{5}$$

In order to always use the most correct version of P in (5), we change from that version of $P(x,y)$ for one domain to that for the next as $x_{100}(t)$ grows from the one domain into the next.

When changing from one version of P to the next it is necessary to re-initialize the droplet distribution at its then current value and continue the solution with the new version of P. The analytic solutions to (1) based on the polynomials in (3) can be evaluated from series expressions given in Scott (1968a) and in Drake and Wright (1972), provided the initial distribution is either a combination of δ-functions or a gamma distribution in x. Because the re-initialized distribution will, in general, not have either of these forms, after the first changeover time it will not be possible to use the series expressions of Scott and of Drake and Wright to obtain $n(x,t)$. It is then necessary to use more general expressions which these workers have derived for arbitrary initial distributions. These expressions are not readily evaluated, however, and because the purpose of this paper is only to show how well analytic solutions to (1) correspond to solutions based on the actual kernel $K(x,y)$ in (2), the analytic solutions have been obtained simply by *numerically integrating* (1). The results will indicate whether an attempt should be made to evaluate $n(x,t)$ using the general expressions.

Each polynomial $P(x,y)$ is fitted to $K(x,y)$ as follows. Because $P(x,y)$ can be written as

$$P(x,y)=\sum_{\substack{m=0\\n=0}}^{\infty} C_{mn}x^m y^n, \tag{6}$$

the condition that it minimize $D(P;K)$ requires the derivative of $D(P;K)$ with respect to each of the potentially non-zero coefficients C_{mn} must equal zero. [These potentially nonzero coefficients would be A, B and C in (3).] This requirement on $D(P;K)$ and the additional stipulation that $P(x,y)$ should have x-y symmetry like the polynomials in (3) together imply that the coefficients C_{mn} minimizing $D(P;K)$ satisfy

$$\frac{\partial D(P;K)}{\partial C_{mn}}+\frac{\partial D(P;K)}{\partial C_{nm}}=0, \quad m\neq n, \tag{7a}$$

$$\frac{\partial D(P;K)}{\partial C_{mm}}=0. \tag{7b}$$

If x-y symmetry is not required the second term in (7a) does not appear, but the additional condition

$$\frac{\partial D(P;K)}{\partial C_{nm}}=0$$

must be included. If symmetry is retained but the polynomial in Eq. (3f) is fitted to K, then in place of (7a) and (7b) must appear equations allowing for the requirement $A=B^2/C$. The remainder of this section assumes polynomials symmetric in x and y. The steps needed for the other types of polynomials should be clear.

Applying (7a) and (7b) to (4) and using (6) yields the following expressions for the minimizing coefficients:

$$C_{mn}=\exp\left\{\frac{\int_S\int \frac{x^m y^n+x^n y^m}{P(x,y)}\ln\left[\frac{K(x,y)}{P_{mn}(x,y)}\right]d(\ln y)d(\ln x)}{\int_S\int \frac{x^m y^n+x^n y^m}{P(x,y)}d(\ln y)d(\ln x)}\right\}, \quad m\neq n, \tag{8a}$$

$$C_{mm}=\exp\left\{\frac{\int_S\int \frac{x^m y^m}{P(x,y)}\ln\left[\frac{K(x,y)}{P_{mm}(x,y)}\right]d(\ln y)d(\ln x)}{\int_S\int \frac{x^m y^m}{P(x,y)}d(\ln y)d(\ln x)}\right\}. \tag{8b}$$

The polynomial $P_{mn}(x,y)$ appearing in Eqs. (8) is defined by

$$P_{mn}(x,y)=P(x,y)/C_{mn}.$$

Eqs. (8) are used in the following way to evaluate each coefficient C_{mn}. First, estimates are made for *all* of the potentially non-zero coefficients in the poly-

TABLE 1. Six symmetric polynomials $P(x,y)$ approximating the actual collection kernel $K(x,y)$.

Approximating polynomial $P(x,y)$	Coefficients minimizing $D(P;K)$ for each droplet pair domain I	II	III	IV	V	Units of coefficient
1. A	$A=1.20\times10^{-4}$ (12)	1.10×10^{-3} (17)	6.46×10^{-3} (22)	3.14×10^{-2} (28)	1.35×10^{-1} (38)	cm^3 sec^{-1}
2. $A+B(x+y)$	$A=0$ $B=8.83\times10^{2}$ (4.8)	0 2.15×10^{3} (4.2)	0 3.28×10^{3} (3.4)	0 4.10×10^{3} (2.9)	0 4.48×10^{3} (2.6)	cm^3 sec^{-1} sec^{-1}
3. Cxy	$C=5.49\times10^{10}$ (4.7)	6.27×10^{10} (5.3)	4.60×10^{10} (7.7)	2.80×10^{10} (13)	1.50×10^{10} (22)	cm^{-3} sec^{-1}
4. $A+B(x+y)+Cxy$ $(A=B^2/C)$	$A=4.41\times10^{-7}$ $B=1.36\times10^{2}$ $C=4.18\times10^{10}$ (4.6)	7.75×10^{-6} 5.05×10^{2} 3.29×10^{10} (4.8)	6.93×10^{-5} 9.51×10^{2} 1.30×10^{10} (5.6)	4.07×10^{-4} 1.23×10^{3} 3.70×10^{9} (6.7)	2.55×10^{-3} 1.45×10^{3} 8.23×10^{8} (8.3)	cm^3 sec^{-1} sec^{-1} cm^{-3} sec^{-1}
5. $A+B(x+y)+Cxy$	$A=0$ $B=4.16\times10^{2}$ $C=2.24\times10^{10}$ (4.5)	0 1.62×10^{3} 6.33×10^{9} (4.0)	0 3.24×10^{3} 8.80×10^{7} (3.4)	0 4.10×10^{3} 0 (2.9)	0 4.48×10^{3} 0 (2.6)	cm^3 sec^{-1} sec^{-1} cm^{-3} sec^{-1}
6. $\sum_{m,n=0}^{2} C_{mn}x^m y^n$	$C_{10}=0$ $C_{01}=C_{10}$ $C_{20}=9.44\times10^{9}$ $C_{02}=C_{20}$ (2.3)	3.46×10^{1} C_{10} 5.28×10^{9} C_{20} (2.4)	1.42×10^{3} C_{10} 5.05×10^{8} C_{20} (2.9)	3.04×10^{3} C_{10} 3.33×10^{7} C_{20} (2.8)	4.04×10^{3} C_{10} 1.70×10^{6} C_{20} (2.6)	sec^{-1} sec^{-1} cm^{-3} sec^{-1} cm^{-3} sec^{-1}

Note: For polynomial 6 those coefficient values not explicitly included in Table 1 were found to converge rapidly toward zero. The parenthetical numbers give $\exp[D(P;K)]$ for each polynomial-domain combination. For example, for polynomial 1-domain I the figure (12) means that throughout domain I, polynomial 1 (in rms terms) is within a factor of 12 of the actual kernel.

nomial. The right-hand sides of (8a) and (8b) are then evaluated (using tenth-order Gauss-Legendre numerical quadrature) for all values of m and n corresponding to the non-zero coefficients. The new estimates obtained for each C_{mn} are then used to reevaluate the right-hand sides of (8a) and (8b) to obtain another estimate for each coefficient. This iterative procedure continues until each coefficient is stationary to at least three significant figures. At the same time $D(P;K)$ is observed and is found to decrease rapidly to a stationary value.

The starting estimate for each coefficient C_{mn} (or C_{mm}) in $P(x,y)$ is obtained from the requirement that the factor $C_{mn}x^m y^n+C_{nm}x^n y^m$ (or $C_{mm}x^m y^m$), when evaluated for $R=50$ μm and $r=10$ μm, be equal to the fraction $1/N$ times the actual value of the kernel for these two droplets. The integer N is chosen equal to the number of distinct coefficients in $P(x,y)$ that are initially permitted to be non-zero [e.g., $N=2$ in (3e)]. This method for selecting the *starting* values of the coefficients is similar to that used by Scott (1968a) in actually evaluating the coefficients A, B and C in Eqs. (3a), (3b) and (3c). Other starting values lead to essentially identical final coefficients.

4. Estimates for $K(x,y)$

The results in Section 5 will be better understood if we develop some estimates as to how the kernel $K(x,y)$ depends on x and y. The collision efficiency can be approximated by

$$E_c(R,r)\approx k_1R^2[1-k_2/r], \quad \text{for} \quad R\lesssim 50\ \mu\text{m},$$

where the factors k_1 and k_2 approximately equal 4.5×10^4 cm^{-2} and 3×10^{-4} cm, respectively. E_c is given by

$$E_c(R,r)\approx 1, \quad \text{for} \quad R\gtrsim 50\ \mu\text{m}.$$

The relative terminal velocity can be expressed by

$$V(R)-V(r)\approx k_3(R^2-r^2), \quad \text{for} \quad R\lesssim 50\ \mu\text{m},$$

where $k_3\approx 1.1\times10^6$ cm^{-1} sec^{-1} and R is in centimeters, and by

$$V(R)-V(r)\approx k_4(R-k_5r^\alpha), \quad \text{for} \quad 50\ \mu\text{m}\lesssim R\lesssim 400\ \mu\text{m},$$

where $k_4\approx 8.5\times10^3$ sec^{-1}. The quantities k_5 and α are both approximately unity for $r\gtrsim 50$ μm, but for smaller r they are approximately 1.3×10^2 cm^{-1} and 2, respectively. Combining these expressions with Eq. (2) yields

$$K(x,y)\approx 9\times10^9[x^{\frac{1}{3}}+y^{\frac{1}{3}}]^2[x^{\frac{2}{3}}(1-k_2'y^{-\frac{1}{3}})][x^{\frac{2}{3}}-y^{\frac{2}{3}}], \quad \text{for} \quad R\lesssim 50\ \mu\text{m}, \quad (9)$$

where $k_2'=(4\pi/3)^{\frac{1}{3}}k_2$, and

$$K(x,y)\approx 6.4\times10^3[x^{\frac{1}{3}}+y^{\frac{1}{3}}]^2[x^{\frac{2}{3}}-k_5'y^{\alpha/3}], \quad \text{for} \quad 50\ \mu\text{m}\lesssim R\lesssim 400\ \mu\text{m}, \quad (10)$$

where $k_5'=(\frac{3}{4}\pi)^{(\alpha-1)/3}k_5$. Eqs. (9) and (10) show that K increases roughly as x^2 for small droplets and as x for larger ones. We also note that K does not depend on y in the same manner as it does on x. It can be expected to increase less strongly with y. In fact, K will decrease as y approaches x. Thus, coefficients of y and y^2 in a polynomial approximating K should be smaller than those for x and x^2. Recalling that each polynomial in (3) has identical coefficients for x and for y, it can

TABLE 2. Three polynomials $P(x,y)$ approximating the actual collection kernel $K(x,y)$.

Approximating polynomial $P(x,y)$	Coefficients minimizing $D(P;K)$ for each droplet pair domain I	II	III	IV	V	Units of coefficient
1. $A+B_1x+B_2y$	$A=0$	0	0	0	0	cm ^{3} sec^{-1}
	$B_1=1.15\times10^3$	2.63×10^3	3.86×10^3	4.68×10^3	5.02×10^3	sec^{-1}
	$B_2=0$	0	0	0	0	sec^{-1}
	(4.1)	(3.6)	(3.0)	(2.6)	(2.3)	
2. $A+B_1x+B_2y+Cxy$	$A=0$	0	0	0	0	cm^3 sec^{-1}
	$B_1=7.91\times10^2$	2.06×10^3	3.73×10^3	4.68×10^3	5.02×10^3	sec^{-1}
	$B_2=0$	0	0	0	0	sec^{-1}
	$C=1.10\times10^{10}$	4.86×10^9	1.78×10^8	0	0	cm^{-3} sec^{-1}
	(4.0)	(3.5)	(3.0)	(2.6)	(2.3)	
3. $\sum_{m,n=0}^{2} C_{mn}x^m y^n$	$C_{10}=0$	1.17×10^2	1.93×10^3	3.67×10^3	4.67×10^3	sec^{-1}
	$C_{20}=1.10\times10^{10}$	5.39×10^9	4.57×10^8	2.91×10^7	1.26×10^6	cm^{-3} sec^{-1}
	(1.9)	(2.2)	(2.6)	(2.5)	(2.3)	

Note: For polynomial 3 those coefficient values not explicitly included in Table 2 were found to converge rapidly toward zero.

be expected that even if the deviation between $K(x,y)$ and these polynomials is minimized by optimizing their coefficients, this minimum will only be relative, compared to that attainable with unrestricted (not symmetric) coefficients. For this reason we have also approximated $K(x,y)$ by polynomials with independent coefficients. This is also in the hope that analytic solutions to (1) may some day be found for them.

5. The approximating polynomials

Tables 1 and 2 display the approximating polynomials for domains I to V.

a. Symmetric volume polynomials

The first five polynomials in Table 1 are those for which (1) can presently be solved analytically. Approximating polynomials of degrees 2, 3, 4 and 5 also were considered, and it was found that they all converge to the sixth polynomial in Table 1 of degree 2. Third-, fourth- and fifth-degree terms evidently play an insignificant role in an approximation to the collection kernel, if domains as large as those considered here are used. Approximating polynomials of degrees six and above were not considered, but they should reduce to the second-degree polynomial.

The parenthetical numbers in Table 1 give exp $\times[D(P;K)]$ for each polynomial. The figure (4.8), for example, means that over the indicated domain there is a 480% rms deviation between $P(x,y)$ and $K(x,y)$. The significance of an error of such magnitude cannot really be assessed without comparing solutions to (1) based on P with those based on K. Section 6 will make this comparison, but it seems clear at this point that polynomials with smaller values of exp$[D(P;K)]$ should lead to more physically realistic solutions to (1). An error of a few hundred percent actually may not be important, since Fig. 1 indicates about a 1000% variation in K itself for a fixed R and varying r.

From Table 1 and Fig. 3 we note that, as expected, the best-fit constant polynomial A [in Eq. (3a)] increases in value as the domain includes larger droplets having larger kernels. Scott's (1968a) value for A is never the best fit to the kernel for any of the domains considered here although it does fit the kernel well for a domain somewhere between I and II.

The second polynomial in Table 1, $A+B(x+y)$ in Eq. (3d), fits $K(x,y)$ best when A is zero. Thus, no improvement to the $B(x+y)$ approximation [in Eq. (3b)] is obtained by adding to it a non-zero constant

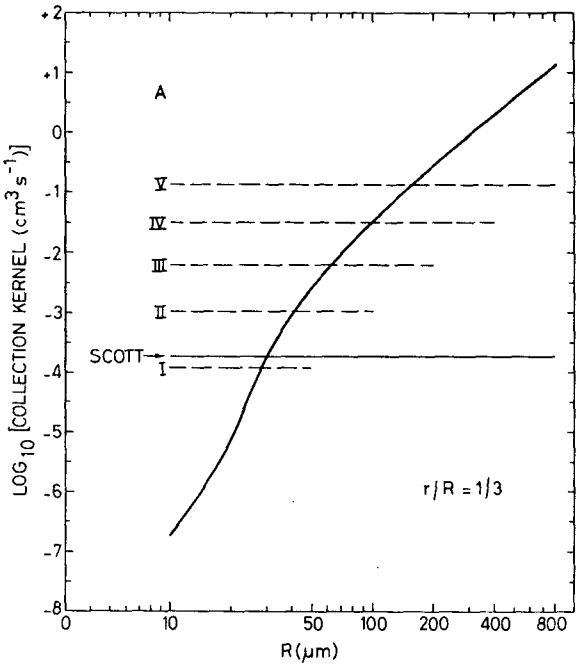

FIG. 3. Comparison of the approximating polynomial A and the actual collection kernel $K(x,y)$ for $r/R=\frac{1}{3}$. Heavy solid line denotes the actual kernel. Light solid line denotes A as proposed by Scott (1968a). Dashed lines denote polynomials determined in this paper and labelled according to domain of approximation.

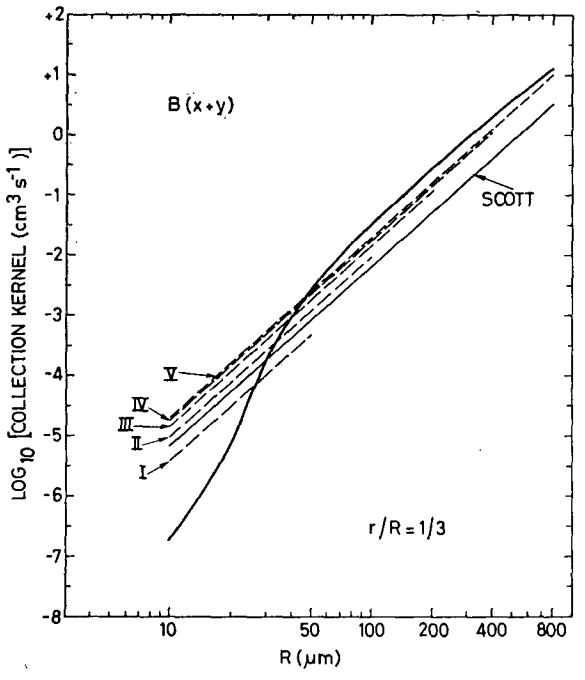

FIG. 4. As in Fig. 3 except for polynomial $B(x+y)$. Light solid line denotes $B(x+y)$ as proposed by Scott (1968a).

factor. This is expected from Eqs. (9) and (10), which indicate that the dominant power of x in any domain considered here lies between x^1 and x^2 and not between x^0 and x^1. Analytic solutions to (1) obtained by Drake and Wright (1972) for $A+B(x+y)$ evidently will be closest to reality if in them A is set equal to zero; hence, the best of these solutions will be those based on the simpler kernel $B(x+y)$. Fig. 4 shows how $B(x+y)$ varies with approximation domain and indicates that Scott's (1968a) choice for B happens to be appropriate for a domain intermediate to II and III. Fig. 5 indicates that for each domain B is smaller than the value of 6000 sec^{-1} proposed by Golovin (1963a). This is because here smaller collector droplets ($R<50$ μm) are also taken into account.

The polynomial Cxy [in Eq. (3c)] is in every case considerably smaller than the candidate proposed by Scott (1968a) (see Fig. 6). This is significant for the validity of analytic solutions to (1) based on this kernel and will be discussed later in this section.

Because the requirement $A=B^2/C$ restricts the range of coefficients in polynomial 4 [in Eq. (3f)] it is a poorer fit to the kernel than the next listed polynomial, $A+B(x+y)+Cxy$, identical except for independent coefficients. Table 1 indicates this latter polynomial fits $K(x,y)$ best when $A=0$. It thus reduces to the polynomial in (3e) for which Drake and Wright (1972)

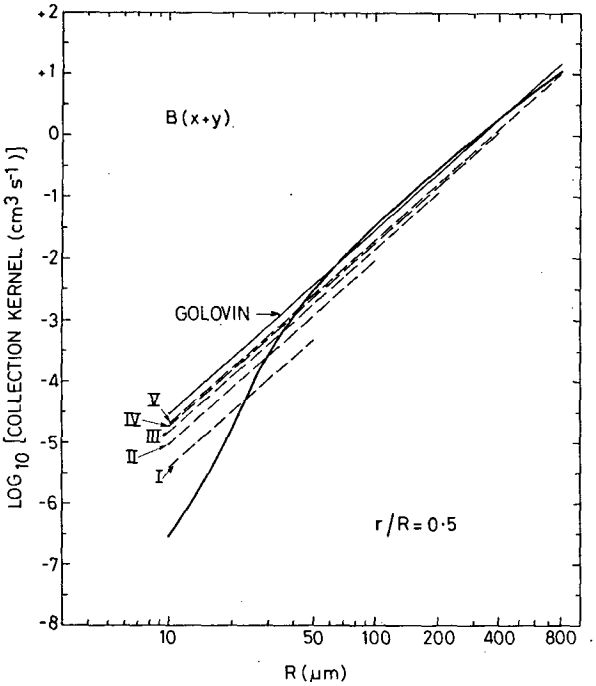

FIG. 5. As in Fig. 4 except for $r/R=0.5$. Light solid line denotes $B(x+y)$ as proposed by Golovin (1963a).

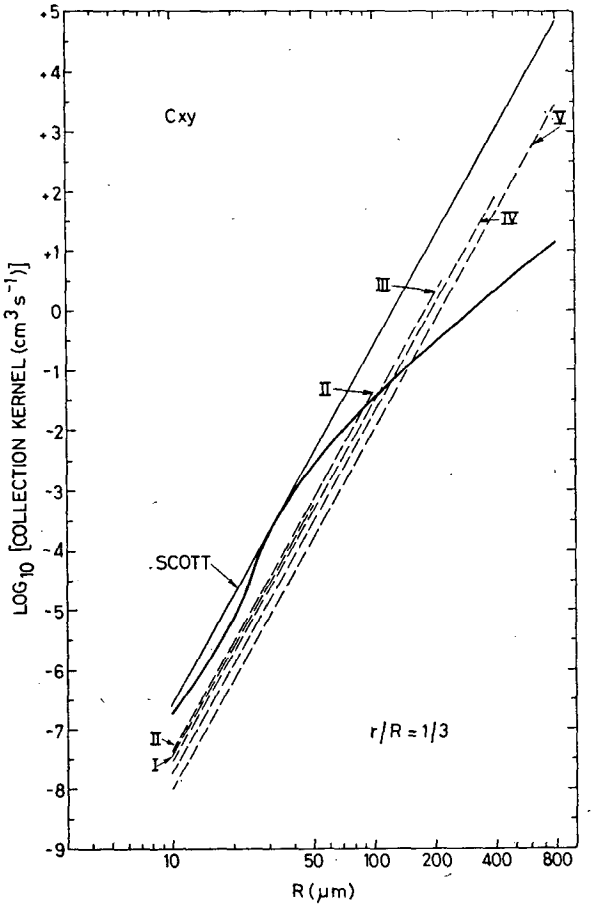

FIG. 6. As in Fig. 3 except for polynomial Cxy. Light solid line denotes Cxy as proposed by Scott (1968a).

have found analytic solutions to (1). Of all those polynomials in Eqs. (3) for which analytic solutions to (1) exist, polynomial 5 is closest to the actual kernel, at least for domains I, II and III. For domains IV and V it is equalled by $B(x+y)$ as the best polynomial. Analytic solutions to (1) based on polynomial 5 should be the most realistic.

The sixth polynomial in Table 1, second degree in x and in y, improves upon the others, most dramatically for domains I, II and III. Figs. 7 and 8 show the relative extent to which it and the polynomials of degree 0 and 1 (first and fifth in Table 1) approximate $K(x,y)$.

The results in Table 1 are consistent with our discussion in Section 4 of the x-dependence expected of K. Polynomial 6 increases with x^2 for small droplets; as the approximation domain includes larger droplets it increases more as the first power of x. Similarly, the coefficient B for the linear terms in polynomials 4 and 5 increases relative to A and C as the approximation domain includes larger droplets. For domain I the coefficient C_{20} in polynomial 6 is similar to the prefactor in Eq. (9). For large domains B in polynomials 2 and 5 is similar to the prefactor in Eq. (10). The factor B is smaller for the polynomials, however, because each allows for collector droplets smaller than 50 μm.

b. Volume polynomials

Table 1 indicates that y plays the same role as x in any polynomial approximating $K(x,y)$. This is only because of the imposed x-y symmetry. Section 4 showed that the smaller droplet actually has a secondary influence on the kernel and suggested that a better approximation to $K(x,y)$ should result if symmetry is not required. Removing x-y symmetry led to the polynomials in Table 2. In every case they approximate $K(x,y)$ better than their counterparts (2, 5 and 6) in Table 1.

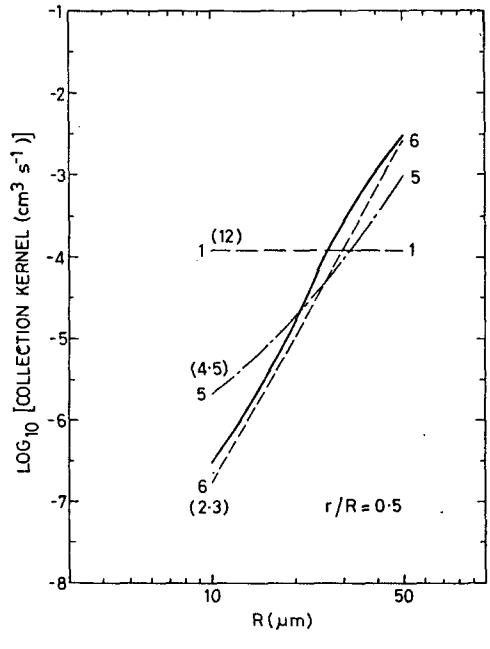

FIG. 7. Comparison for domain I of the actual kernel and the polynomials 1, 5 and 6 in Table 1 of orders 0, 1 and 2, respectively. Parenthetically attached to each graph is its rms deviation $\exp[D(P;K)]$ from the actual kernel.

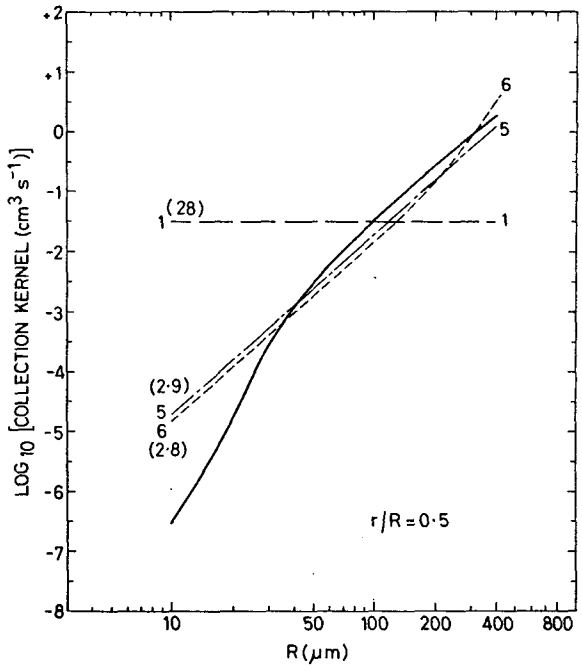

FIG. 8. As in Fig. 7 except for domain IV.

This does not imply no y-dependence in the kernel but simply indicates that on the scale of the approximation domains used here and to within the resolution provided by integer powers of x and y, any polynomial potentially having some terms involving only y approximates $K(x,y)$ best if these terms are all zero. The gross behavior of $K(x,y)$ is thus determined only by the size of the larger, collector droplet. This is not surprising, since Fig. 1 indicates the kernel changes by several orders of magnitude as x varies over its natural range but varies by only about one order of magnitude as y varies over its range.

c. Piecewise approximations to K

Figs. 5 and 7 indicate $K(x,y)$ may be closely approximated by two separate polynomials, one for domain I where K behaves as x^2 and another for that portion of domain V exterior to domain I where it behaves as x. Polynomial 6 in Table 1 or polynomial 3 in Table 2 can serve as the domain I approximation. The Golovin polynomial would be suitable for the larger droplets but can be improved slightly using the techniques of Section 3. The following two piecewise approximations

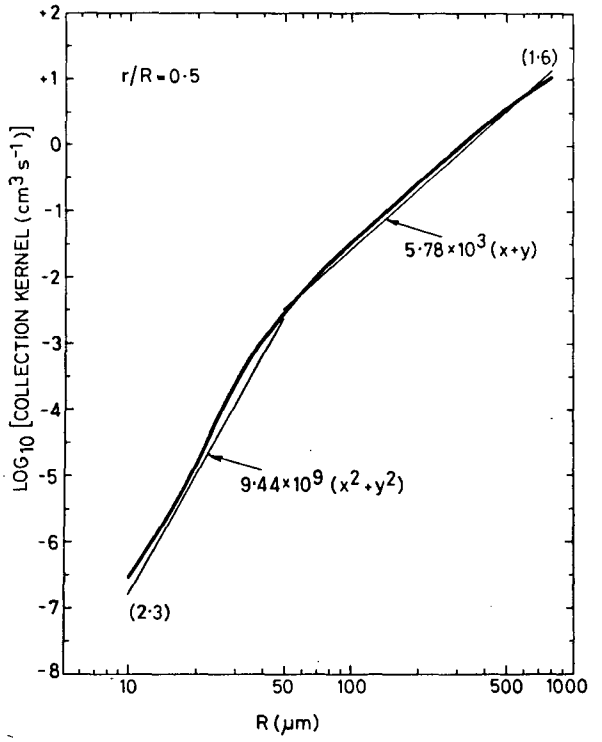

FIG. 9. Comparison of the approximating polynomial in (11) and the actual kernel. The parenthetical numbers give $\exp[D(P;K)]$ for the two parts of the polynomial, fitted over domain I and over that portion of domain V exterior to domain I.

to K have thus been obtained:

$$P(x,y)=9.44\times10^{9}(x^2+y^2);\quad \exp[D(P;K)]=2.3,\quad \text{for } R\leqslant 50\,\mu\text{m} \tag{11a}$$

$$P(x,y)=5.78\times10^{3}(x+y);\quad \exp[D(P;K)]=1.6,\quad \text{for } R>50\,\mu\text{m} \tag{11b}$$

and

$$P(x,y)=1.10\times10^{10}x^2;\quad \exp[D(P;K)]=1.9,\quad \text{for } R\leqslant 50\,\mu\text{m} \tag{12a}$$

$$P(x,y)=6.33\times10^{3}x;\quad \exp[D(P;K)]=1.4,\quad \text{for } R>50\,\mu\text{m}. \tag{12b}$$

The approximation in (11) is displayed in Fig. 9. Whether the collection equation can be solved analytically using these piecewise approximations is an open question because some of the mathematical techniques heretofore used are not applicable. Nevertheless, the small values of $\exp[D(P;K)]$ for both approximations indicate the merit in searching for such solutions. Section 6 will show how well numerical solutions to (1) based on these approximations correspond to solutions based on the actual kernel.

d. Validity of the xy term

Tables 1 and 2 show that for the smaller domains as terms of higher degree are included in a polynomial it approximates K better. This is consistent with Section 4, where estimates of the x and y dependence of K were made. Drake (1972) has argued, on the other hand, that any polynomial containing an xy term or terms increasing as fast as xy is probably a poor approximation to the collection kernel. Drake's argument is based on the observation that if the kernel has the form Cxy then there is a time τ given by

$$\tau=[CM_2(t_0)]^{-1}, \tag{13}$$

where $M_2(t_0)$ is the initial value of the second-order moment of $n(x,t)$, such that for $t\geqslant\tau$ solutions to the collection equation based on Cxy become meaningless. In particular, as $t\to\tau$, $M_2(t)\to+\infty$, and for $t>\tau$ liquid water is no longer conserved (McLeod, 1964). Drake also shows that if the kernel has the form $A+B(x+y)+Cxy$, where $A=B^2/C$, then

$$\tau=[CM_2(t_0)+BL]^{-1}, \tag{14}$$

where L is the liquid water content of the droplets. If the kernel has the form $B(x+y)+Cxy$ then τ is given by

$$\tau=\ln[1+2BL/CM_2(t_0)]/(2BL). \tag{15}$$

In evaluating τ in (13) Drake (1972) used a realistic value for $M_2(t_0)$ but for C he used Scott's (1968a) value of 3.8×10^{11} cm^3 sec^{-1}. This is considerably larger than the corresponding domain I (small droplet) value given in Table 1. Drake's τ of 315 sec is thus considerably smaller than the 2200 sec predicted here. Eqs. (14) and (15) can also be used to evaluate τ. One might assume, using the same rationale as Scott (1968a), that for the (30 μm, 10 μm) droplet pair the constant, linear, and quadratic terms in $A+B(x+y)+Cxy$ each equal one-third the actual kernel, and the linear and quadratic terms in $B(x+y)+Cxy$ each equal one-half the actual kernel. For $L=10^{-6}$ cm^3 of water per cubic centimeter of air this implies τ in (14) is 630 sec and τ in (15) is 440 sec. These times are also smaller than the respective times of 2100 sec and 2000 sec obtained using B and C in Table 1.

It is easy to understand why solutions to (1) based on polynomials containing an xy term may be valid only for $t\leqslant\tau$. This can be understood even though these polynomials approximate K better than polynomials of lower degree, such as $B(x+y)$, which yield solutions valid at all times. The following expression is simply derived from (1) and shows how the kernel affects $M_2(t)$:

$$\frac{dM_2(t)}{dt}=\int_0^\infty yn(y,t)\int_0^\infty xn(x,t)K(x,y)\,dx\,dy. \tag{16}$$

Any kernel containing an xy term will predict an infinite value for $M_2(t)$ at some finite $t=\tau$. For $B(x+y)$, on the other hand, $M_2(t)$ will exponentially increase with time but still be finite at any finite time. Physically, the xy term predicts too rapid growth for the

large drops in a cloud. For example, Cxy is fairly close to $K(x,y)$ in domain I (see Fig. 6), but if it is extrapolated to sufficiently larger droplet sizes it will be many times larger than K. An extrapolation of this type occurs in Eq. (16) in extending the integration variables x and y beyond domain I. This is not important so long as there are no droplets beyond domain I (τ is thus positive) but, once these exist, because Cxy is too large they will grow too rapidly and $M_2(t)$ will become too large. It will become infinite at $t=\tau$. The same behavior will occur using any polynomial with an xy (or an x^2) term.

The restriction to times $t \leqslant \tau$ (or, alternatively, to the poorer first-degree polynomials) is avoided here by changing from one version of a polynomial to the next as the droplets grow. This procedure (see Section 3) is designed so that $P(x,y)$ for the 100th-largest droplet is similar to $K(x,y)$ in (2). Because K behaves linearly with x for $R>50$ μm, $P(x,y)$ will behave more linearly as the changeover from one version to the next occurs, and τ will either be pushed back or made infinite. Specifically, by changing from one version to the next of a polynomial containing Cxy, a smaller value of C will come into effect (see Tables 1 and 2), the linear term $B(x+y)$ or B_1x will predominate, and $M_2(t)$ will behave more as an exponentially increasing function than as one going to infinity in a finite time. The closer to exponential its behavior becomes the longer and less restrictive τ will become. If $C \rightarrow 0$, the behavior will become exactly exponential, τ will become infinite, and no restriction will exist at all. (This will occur for polynomial 5 in Table 2 once the domain IV version comes into effect.) The results in the next section show that the restriction to $t \leqslant \tau$ is indeed avoided by changing from one version to the next as the droplets grow.

6. Solutions to the collection equation

Solutions to (1) have been obtained using several of the better approximations in Tables 1 and 2. This section compares these solutions with those based on the actual kernel in (2). The polynomials used are 2, 5 and 6 in Table 1, all those in Table 2, and those in Eqs. (11) and (12). Analytic solutions to (1) have been found to date only for polynomials 2 and 5 in Table 1. The remaining polynomials more closely approximate $K(x,y)$, however, and on the basis of the results in this section it will be suggested that analytic solutions be sought for some of them.

In every case, the collection equation is solved by numerical integration. The reasons for this have been discussed in Section 3. The numerical techniques used are essentially those developed by Reinhardt (1972) and can be trusted to yield reliable answers. As already stated, when solving (1) using any given polynomial [except those in (11) and (12)] we change from one version to the next according to the size of the 100th-largest drop. The supposition in Section 5 that this would extend the period of validity of the solutions could be explicitly confirmed for the $B(x+y)+Cxy$ polynomial (see Table 3). It was implicitly confirmed for most of the other polynomials by noting that throughout the period of integration (from 0 to 1800 sec) liquid water was conserved, at least within the errors of the numerical process. McLeod (1964) has shown for the Cxy kernel that once τ is surpassed L is no longer conserved. When using polynomials 6 in Table 1 and 3 in Table 2 liquid water was not conserved in the maritime cloud after about 350 sec and in the continental cloud after about 650 sec. These polynomials thus yield valid solutions to (1) only in the early stages of a cloud's evolution. Even though the domain I versions of polynomials 6 and 3 are partly incorporated in (11) and (12) for these approximations liquid water was conserved at all times. This is because (11) and (12) better describe the kernel at large droplet sizes.

TABLE 3. Comparison of T and $T+\tau$ for the polynomial $B(x+y)+Cxy$: T is the changeover time from the current version of the polynomial to the next, and $T+\tau$ the period of validity of a solution to (1) based on the current version. All values are in seconds.

	Domain of current version				
	I	II	III	IV	V
T	335	800	1205	1545	
$T+\tau$	1049	1108	1659	∞	∞

In each case the initial distribution has the well-known form

$$n(x,t_0)=\frac{N^2(t_0)}{L}\frac{(\nu+1)^{\nu+1}}{\Gamma(\nu+1)}\left(\frac{x}{x_0}\right)^{\nu}e^{-(\nu+1)x/x_0}. \qquad (17)$$

In (17) $N(t_0)$ is the initial number density of droplets of all sizes and equals 50 cm^{-3} (maritime clouds) or

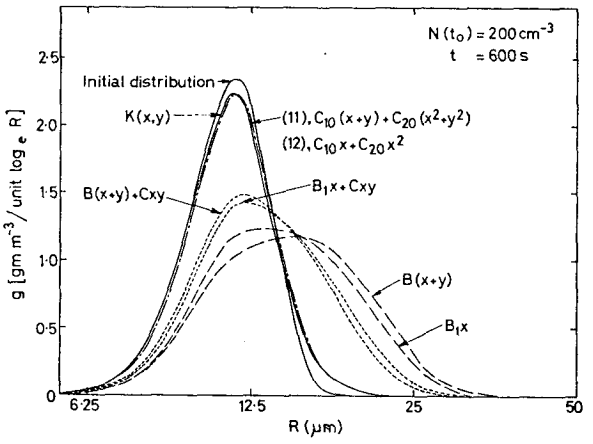

FIG. 10. Liquid water distribution at 600 sec in a typical continental cloud, as predicted by the actual collection kernel $K(x,y)$ in (2) and as predicted by various polynomials approximating K.

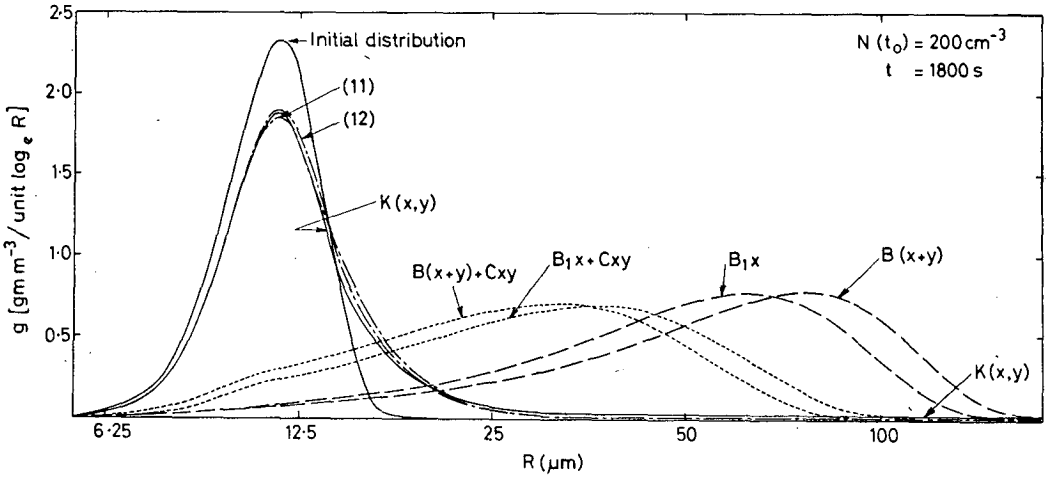

FIG. 11. As in Fig. 10 except at 1800 sec.

200 cm^{-3} (continental clouds); and L is the liquid water content of all the droplets taken together and equals 10^{-6} cm^3 of water per cubic centimeter of air. The parameter ν is given by

$$\nu = D_x^{-2} - 1,$$

where D_x is the relative dispersion in x. A value of $\nu = 2$ is used here, for which $D_x \approx 0.58$ and $D_r \approx 0.20$.

a. Continental cloud

Figs. 10–12 show how the distribution of liquid water among the droplets, $g(\ln R,t) \equiv 3x^2 n(x,t)$, changes with time, and how the 100th-largest drop grows. There is little meaningful difference between predictions based on the symmetric polynomials in Table 1 and Eq. (11) and on their slightly better counterparts in Table 2 and Eq. (12). There is a significant difference, which is now discussed, between the predictions based on the linear polynomials and those containing an xy term and the predictions based on (11), (12) and the polymials having x^2 terms.

The linear polynomials and those containing xy predict a general collapse of the distribution into a smaller number of larger droplets. This occurs because these polynomials are 10–20 times too large at just those radii ($\sim$10 μm) where most cloud droplets are initially located (cf. Figs. 5, 7 and 10). Following the initial collapse, the distribution moves to the right and for some time maintains a tail extending beyond that of the actual distribution (see Fig. 12). Eventually, however, the predicted kernel for the droplets in the tail becomes smaller than the actual kernel (see Figs. 5 and 7), their growth rate is slowed compared to the droplets in the tail of the actual distribution, and these droplets become as large.

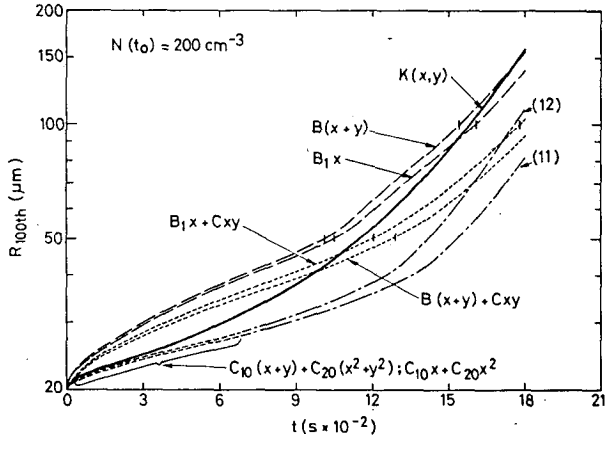

FIG. 12. The radius of the 100th-largest droplet per cubic meter of a typical continental cloud, as predicted by the actual collection kernel $K(x,y)$ in (2) and as predicted by various polynomials approximating K. Vertical strokes on graphs denote the time when a change is made from one version of a polynomial to the next. Braces show period of validity of results (short-dashed lines) obtained using the indicated polynomials. These results are here virtually identical to those obtained using (11) and (12).

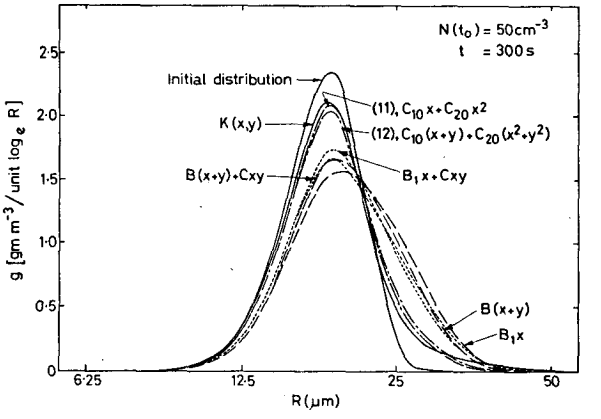

FIG. 13. Liquid water distribution at 300 sec in a typical maritime cloud, as predicted by the actual collection kernel $K(x,y)$ in (2) and as predicted by various polynomials approximating K.

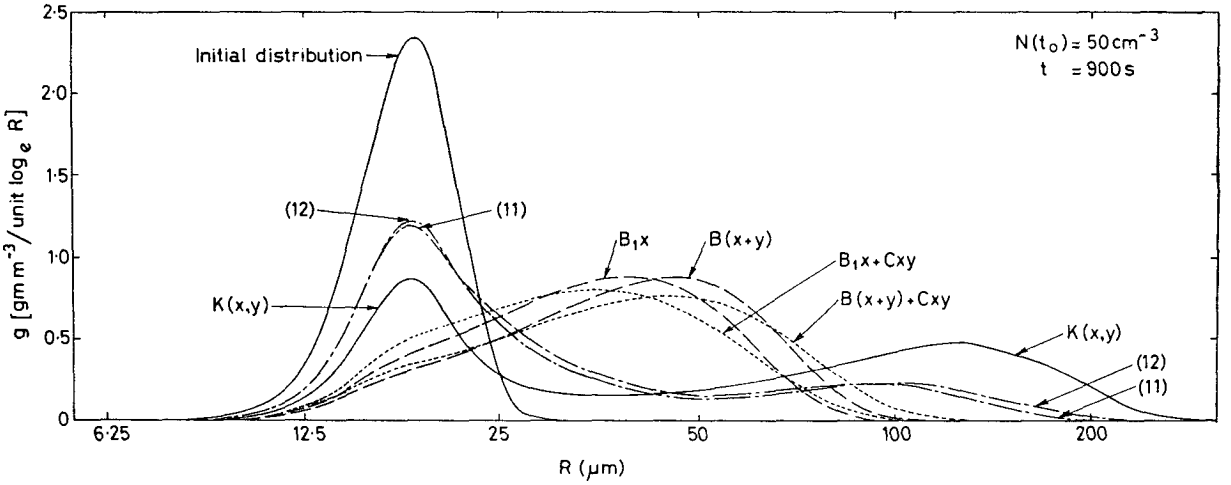

FIG. 14. As in Fig. 13 except at 900 sec.

The polynomials containing x^2 and the approximations in (11) and (12), on the other hand, predict a liquid water distribution remarkably similar to the actual distribution. This can be attributed to the much better approximation to K in domain I where all the droplets initially lie. The development of the distribution is thus not biased by an initial collapse and instead proceeds in the expected manner. The initial peak in the distribution slowly decreases, a tail is formed toward the larger sizes, and there is only a few minutes' difference in the time needed for $R_{100}(t)$ to equal 100 μm, the size of a fine drizzle droplet. These similarities exist even though there is a 100–150% error in the approximations in domain I and a 40–60% error for larger droplets. A breakdown of $K(x,y)$ into linear and quadratic parts apparently retains most of the physics originally contained in the collision efficiencies and terminal velocities.

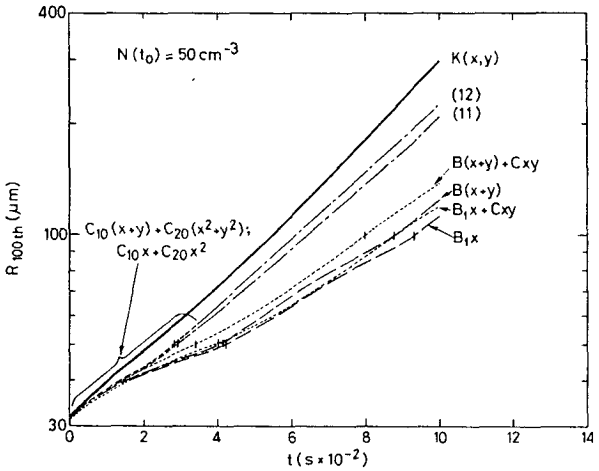

FIG. 15. The radius of the 100th-largest droplet per cubic meter of a typical maritime cloud. Legend is otherwise identical to that in Fig. 12.

b. Maritime cloud

Fig. 13 shows, for this cloud and for the linear polynomials and those containing xy, a smaller relative collapse of the spectrum. This is expected because, first, there are now fewer droplets initially, thus fewer collection events, and second, the droplets that do exist initially are located around 18 μm, where the polynomials are less in error (see Figs. 5 and 7).

As in the continental cloud there is a better correspondence between the actual distribution and that predicted by the polynomials in (11) and (12). The second maximum in $g(\ln R)$ noted by Berry (1967) appears for the approximating polynomials as well (Fig. 14) and the 100th-largest drop takes only 10–15% longer to reach any given size (Fig. 15). Once again, an x^2 (small collector droplet) and x (large collector droplet) dependence in K describes its essential features.

7. Conclusions

Numerical solutions to the droplet collection equation, using certain polynomial approximations to the gravitational collection kernel, have been examined to learn whether they usefully describe the evolution of a cloud droplet distribution. The results for typical continental and maritime clouds (Figs. 10–15) show that the distribution is closely described if the actual kernel $K(x,y)$ is replaced by

$$\begin{aligned} &9.44\times10^{9}(x^2+y^2), \quad R\leqslant 50\ \mu\text{m} \\ &5.78\times10^{3}(x+y), \quad R>50\ \mu\text{m} \end{aligned}$$

[see Eq. (11) and Fig. 9] or by

$$\begin{aligned} &1.10\times10^{10}x^2, \quad R\leqslant 50\ \mu\text{m} \\ &6.33\times10^{3}x, \quad R>50\ \mu\text{m} \end{aligned}$$

[see Eq. (12)]. R is the radius of the larger droplet, x is its volume in cubic centimeters, and y is the volume of the smaller droplet.

From the standpoint of including droplet collection in multi-dimensional cloud models, an analytic solution to the collection equation is desirable. An attempt should be made to find such solutions based upon either of the above approximations. If these cannot be found because of the piecewise nature of the approximations, then solutions based on the portions for $R<50\,\mu$m still would describe the first few hundred seconds of droplet growth. A comparatively poor description of the droplet distribution comes from the most physically realistic analytic solution presently existing, i.e., based on the kernel approximation $B(x+y)+Cxy$.

Acknowledgments. The research reported here was initially supported at CSIRO by a National Science Foundation Postdoctoral Fellowship.

REFERENCES

Beard, K. V., and H. R. Pruppacher, 1969: A determination of the terminal velocity and drag of small water drops by means of a wind tunnel. *J. Atmos. Sci.*, **26**, 1066–1072.

Berry, E. X, 1965: Cloud droplet growth by collection: A theoretical formulation and numerical calculation. Ph.D. dissertation, University of Nevada, Reno.

——, 1967: Cloud droplet growth by collection. *J. Atmos. Sci.*, **24**, 688–701.

——, 1968: Comments on "Cloud droplet coalescence: Statistical foundations and a one-dimensional sedimentation model." *J. Atmos. Sci.*, **25**, 151–152.

Bleck, R., 1970: A fast, approximative method for integrating the stochastic coalescence equation. *J. Geophys. Res.*, **75**, 5165–5171.

Brazier-Smith, P. R., S. G. Jennings and J. Latham, 1972: The interaction of falling water drops: Coalescence. *Proc. Roy. Soc. London*, **A326**, 393–408.

Drake, R. L., 1972: The scalar transport equation of coalescence theory: Moments and kernels. *J. Atmos. Sci.*, **29**, 537–547.

——, and T. J. Wright, 1972: The scalar transport equation of coalescence theory: New families of exact solutions. *J. Atmos. Sci.*, **29**, 548–556.

Enukashvili, I. M., 1964a: On the solution of the kinetic coagulation equation. *Bull. Acad. Sci. USSR, Geophys. Ser.*, No. 10, 944–948.

——, 1964b: On the problem of a kinetic theory of gravitational coagulation in spatially heterogeneous clouds. *Bull. Acad. Sci. USSR, Geophys. Ser.*, No. 11, 1043–1045.

Foote, G. B., and P. S. du Toit, 1969: Terminal velocity of raindrops aloft. *J. Appl. Meteor.*, **8**, 249–253.

Gillespie, D. T., 1972: The stochastic model for cloud droplet growth. *J. Atmos. Sci.*, **29**, 1496–1510.

Golovin, A. M., 1963a: The solution of the coagulation equation for cloud droplets in a rising air current. *Bull. Acad. Sci. USSR, Geophys. Ser.*, No. 5, 482–487.

——, 1963b: On the spectrum of coagulating cloud droplets. II. *Bull. Acad. Sci. USSR, Geophys. Ser.*, No. 9, 880–884.

——, 1963c: On the kinetic equation for coagulating cloud droplets with allowance for condensation. III. *Bull. Acad. Sci. USSR, Geophys. Ser.*, No. 10, 949–953.

——, 1965: Kinetics of cloud droplets in a model of stationary axisymmetrical cumulus clouds. *Bull. Acad. Sci. USSR, Atmos. Oceanic Phys. Ser.*, **1**, No. 7, 422–426.

Gunn, R., and G. D. Kinzer, 1949: The terminal velocity of fall for water droplets in stagnant air. *J. Meteor.*, **6**, 243–248.

Klett, J. D., and M. H. Davis, 1973: Theoretical collision efficiencies of cloud droplets at small Reynolds numbers. *J. Atmos. Sci.*, **30**, 107–117.

Long, A. B., 1971: Validity of the finite-difference droplet collection equation. *J. Atmos. Sci.*, **28**, 210–218.

——, 1972a: Reply (to Comments by Scott). *J. Atmos. Sci.*, **29**, 594–595.

——, 1972b: A theoretical investigation of the evolution of a cloud droplet population as determined by collision and coalescence. Ph.D. dissertation, University of Arizona, Tucson.

——, and M. J. Manton, 1974: On the evaluation of the collection kernel for the coalescence of water droplets. *J. Atmos. Sci.*, **31**, 1053–1057.

McLeod, J. B., 1964: On the scalar transport equation. *Proc. London Math. Soc.*, **14**, 445–458.

Melzak, Z. A., 1953: The effect of coalescence in certain collision processes. *Quart. J. Appl. Math.*, **11**, 231–234.

Reinhardt, R. L., 1972: An analysis of improved numerical solutions to the stochastic collection equation for cloud droplets. Ph.D. dissertation, University of Nevada, Reno.

Scott, W. T., 1967: Poisson statistics in distributions of coalescing droplets. *J. Atmos. Sci.*, **24**, 221–225.

——, 1968a: Analytic studies of cloud droplet coalescence. I. *J. Atmos. Sci.*, **25**, 54–65.

——, 1968b: Comments on "Cloud droplet coalescence: Statistical foundations and a one-dimensional sedimentation model." *J. Atmos. Sci.*, **25**, 150.

——, 1972: Comments on "Validity of the finite-difference droplet collection equation." *J. Atmos. Sci.*, **29**, 593–594.

Shafrir, U., and T. Gal-Chen, 1971: A numerical study of collision efficiencies and coalescence parameters for droplet pairs with radii up to 300 microns. *J. Atmos. Sci.*, **28**, 741–751.

Twomey, S., 1964: Statistical effects in the evolution of a distribution of cloud droplets by coalescence. *J. Atmos. Sci.*, **21**, 553–557.

——, 1966: Computations of rain formation by coalescence. *J. Atmos. Sci.*, **23**, 405–411.

Warshaw, M., 1967: Cloud droplet coalescence: Statistical foundations and a one-dimensional sedimentation model. *J. Atmos. Sci.*, **24**, 278–286.

——, 1968a: Reply (to Comments by Scott and Berry). *J. Atmos. Sci.*, **25**, 152–154.

——, 1968b: Cloud droplet coalescence: Effect of the Davis-Sartor collision efficiency. *J. Atmos. Sci.*, **25**, 874–877.

Whelpdale, D. M., and R. List, 1971: The coalescence process in raindrop growth. *J. Geophys. Res.*, **76**, 2836–2856.

Woods, J. D., and B. J. Mason, 1964: Experimental determination of collection efficiencies for small water droplets in air. *Quart. J. Roy. Meteor. Soc.*, **90**, 373–381.